

Robot-mediated asymmetric connection between humans can improve performance without increasing effort

Alessia Noccaro^{1,2}, Silvia Buscaglione², Jonathan Eden^{3,4}, Cheng Xiaoxiao³, Nicola Di Stefano⁵, Giovanni Di Pino², Etienne Burdet³, and Domenico Formica^{1,2}

¹School of Engineering, Neurorobotics Lab, Newcastle University

²NEXT: Neurophysiology, Neuroengineering of Human-Technology Interaction Research Unit, Università Campus Bio-Medico di Roma

³Department of Bioengineering, Imperial College of Science Technology and Medicine

⁴Mechanical Engineering Department, University of Melbourne

⁵Institute of Cognitive Sciences and Technologies (ISTC), National Research Council (CNR)

December 22, 2023

Robot-mediated asymmetric connection between humans can improve performance without increasing effort

Alessia Nocco^{1,2†*}, Silvia Buscaglione^{2†}, Jonathan Eden^{3,4}, Cheng Xiaoxiao³, Nicola Di Stefano⁵, Giovanni Di Pino², Etienne Burdet³, and Domenico Formica^{1,2*}

¹Neurorobotics Lab, School of Engineering, Newcastle University, UK

²NEXT: Neurophysiology and Neuroengineering of Human-Technology Interaction Research Unit, Università Campus Bio-Medico di Roma, Italy.

³ Department of Bioengineering, Imperial College of Science Technology and Medicine, London, UK.

⁴ Mechanical Engineering Department, University of Melbourne, Victoria, Australia,

⁵ Institute of Cognitive Sciences and Technologies (ISTC), National Research Council (CNR), Rome, Italy

† Equal contribution

* E-mail: {alessia.nocco, domenico.formica}@newcastle.ac.uk

Abstract—Rationale: Whether working together to move a table or supporting a child learning to ride a bike, physically connected individuals use the exchange of haptic information to improve motor performance. However, this improvement occurs at the cost of additional effort for the more skilled partner. **Objective:** Here, we aim to assess whether an asymmetric connection, consisting of a stiffer link to the less skilled partner, could increase performance without additional effort in collaborative tasks. **Methods:** Through computational modelling, we first evaluated such a hypothesis on simulated human dyads tracking a common target. The approach was then experimentally validated on a three degree-of-freedom tracking task using two commercial robots as individual interfaces. **Results:** The simulation and experimental results confirm that using an asymmetric connection stiffness can improve joint performance without requiring additional effort from either partner compared to solo performance. **Conclusion:** This suggests that the training of motor skills with a proficient partner – like a physical therapist assisting a patient or a violin teacher demonstrating bowing techniques – may be enhanced through the use of robot-mediated asymmetric haptic communication.

Index Terms—Human-robot interaction, joint action, human motor control

Impact Statement—Using an asymmetric connection in a dyad enables the partners to improve their common performance without additional effort.

I. INTRODUCTION

Humans perform collaborative tasks in a wide range of everyday actions [1], [2], [3], [4], [5], [6], [7], [8], from moving furniture together or tango dancing, to more asymmetric collaborations such as a therapist assisting a patient in physical training or a violin teacher holding their student’s arm to demonstrate how to perform bowing movements. These collaborations rely on *haptic communication* where recent results suggest that the exchange of haptic information between connected humans improves the performance of both partners [9], [10], [11] and their motor learning [12]. In addition to enabling

haptic communication, the mechanical connection guides the less skilled person with a better performing trajectory but also deviates the more skilled one from the target. Importantly, the improvement of both partners’ performance comes at the cost of a higher effort for the better one [13].

Could this effort-performance trade-off from two partners performing a task together be improved by making the more skilled partner have a larger influence on the coupled movement? In direct human-human interactions, the forces of both partners oppose each other, as expressed by Newton’s third law. However, connecting for instance a physiotherapist and a patient via personal robotic interfaces enables the implementation of an asymmetric interaction, where the less skilled partner is stiffly connected to the more skilled partner’s movement, who feels little resistance from a soft connection to the less skilled partner. This can be achieved through the use of a robot-mediated connection between the partners (see Fig. 1A). Our hypothesis is that the stiff connection will provide the less skilled partner with good guidance and haptic information, while the softer connection will still provide the more skilled partner with haptic information but attenuate the perturbing force, thus reducing the additional effort required for accurately controlling the movement.

To test this hypothesis, we consider a task where two partners have to track a common moving target. Modulating the tracking performance using visual noise, the interaction force can be regulated by an asymmetric connection stiffness, so that a better performing partner can exert higher force on the other. Assuming that a user obtains information about their partner’s motion plan through haptic communication, which they combine with their visual information of the target [14], [13], we first simulated this strategy with both symmetric and asymmetric stiffness. The predictions from the model were then tested in an experiment using both symmetric and asymmetric connections with 20 healthy participants (grouped in 10 *dyads*), modulating their motor skill using visual noise

[13]. In contrast to previous studies that tested with high-performance haptic interfaces in horizontal tasks with only one or two degrees-of-freedom (DoFs) [10], [14], [13], [11], our task involved three DoFs and gravity. It was also implemented using two commercial robots (see Fig. 1B), thereby validating its suitability for more realistic use cases.

II. RESULTS

A. Simulated asymmetric stiffness behaviour

To simulate the effect of asymmetric stiffness on human-human physical interaction, we extended the model of haptic communication, developed in [13], for one DoF tracking and symmetric stiffness. This model is based on four principles: i) each partner’s central nervous system (CNS) realises that the haptic feedback signal it receives is related to the visual tracking task; ii) using an impedance model of the partner’s control, the CNS then extracts the partner’s target from the interaction; iii) it combines its own and the partner’s targets in a stochastic optimal way, yielding Bayesian sensor fusion across the haptic channel; iv) the haptic connection with the partner is considered as a source of additive noise, where a more compliant connection has a larger deviation than a stiff one. To create an asymmetric connection with different stiffness levels for the two partners, we modified ii) by increasing the interaction stiffness gain from the more skilled partner to the less skilled one and decreasing the stiffness gain from the less to the more skilled partners (Fig. 1A). This also increases the more skilled partner’s influence on the target estimation of the less skilled partner.

This model was tested through a simulation of the tracking of a randomly moving target in the three DoFs (x, y, φ) of translation and rotation in a vertical plane (Fig. 1B). To examine the influence of the tracking skill, one participant of each dyad had a higher amount of visual noise (Fig. 1C), which increased their tracking error (Fig. 1D). The other partner had small amount of visual noise and was thus “more skilled” as they had a smaller tracking error. The simulation consisted of 160 connected dyadic trials and alternated 160 disconnected “solo” trials. Here, connected trials were conducted using low (L: $\{K_x = K_y = 60 \text{ N/m}, K_\varphi = 3 \text{ Nm/rad}\}$) and high (H: $\{K_x = K_y = 180 \text{ N/m}, K_\varphi = 9 \text{ Nm/rad}\}$) stiffness levels independently for each partner. This resulted in two symmetric $\{\text{HH}, \text{LL}\}$ and two asymmetric $\{\text{HL}, \text{LH}\}$ scenarios, where the first stiffness listed in the dyad corresponds to the one felt by the more skilled partner.

To evaluate the change in performance between connected and solo trials, we computed the *improvement of tracking error* $I = 1 - e_c/e$ with connection, where e_c is the root mean square tracking error in a connected trial and e the error in the previous solo trial. The improvement (Fig. 2A) was affected by the stiffness scenario (Friedman test, $\chi^2 = 148, p < 0.001$), with the highest improvement for the asymmetric LH case (all comparisons $p < 0.001$) and lowest improvement for the HL case (all $p < 0.001$).

The overall change in effort required by connected trials with respect to solo trials was also evaluated, through the root mean square α of the simulated motor command. The change

of this parameter with connection, computed as $A = \alpha_c/\alpha - 1$, is depicted in Fig. 2B with respect to the *partner’s relative error* $E = 1 - e_p/e$. The stiffness affected the *interaction effort* (Friedman test, $\chi^2 = 53, p < 0.001$). The HH and HL scenarios resulted in the highest participant effort, whereas lower effort was observed in the LH condition and even less in the LL case [$\text{HH} = \text{HL} > \text{LH} (p < 0.001) > \text{LL} (p = 0.006)$]. We fitted data through linear-mixed effect models considering the *improvement* (or the *effort*) as the dependent variable, the *partner’s relative error* as predictors and the dyads as a random variable. The goodness of fitting resulted in R^2 equal to 0.91 (HH), 0.87 (LL), 0.87 (HL), 0.93 (LH) for the *improvement* and R^2 equal to 0.18 (HH), 0.078 (LL), 0.49 (HL), 0.055 (LH) for the *effort*. Here, low values for the fitting (as observed for the LH condition) indicate that there is no correlation between the effort and the partner’s skill such that the effort is balanced between partners.

In summary, simulation with our model of haptic communication suggests that asymmetric stiffness enables the reduction of tracking error without an effort increase through the LH scenario. Considering the *trade-off* between improvement and interaction effort $TO = (I+1)/(A+1)$ (Fig. 2C), LH appears to be the optimal configuration, as for this measure $\text{LH} > \text{LL} > \text{HH} > \text{HL}$ (all $p < 0.001$).

B. Human-human experiments

Do physically interacting human-human dyads show similar behaviour when connected through asymmetric stiffness as predicted by our model? To test this, 20 healthy volunteers (aged 22.5 ± 2.6 years old, 9 female, 18 right-handed) participated in an experiment using the same tracking task as described above. Participants provided written informed consent, and were then paired in ten dyads with the same handedness (assessed through [15]). Each participant sat with a robot arm on their dominant hand side. The robot arm was programmed to move in a vertical plane in front of them and compensate for its own gravity. A monitor in front of them displayed a target moving in the vertical plane and a cursor corresponding to their hand movement (Fig. 1B). They were separated from their partner by a curtain and were not aware of the task performed by the partner, nor of a possible physical connection with them. Figure 3A depicts the two session experimental protocol, with each session composed of three phases: familiarization, baseline, and test. The *test phase* consisted of alternated trials with and without the physical connection, with in total 40 trials with connection and 40 without, where the stiffness conditions were pseudo-randomized among the connected trials. One participant of each dyad had a cloudy target with Gaussian visual noise [13] (Fig. 1C), while the other partner had a sharp target. On the second day, the partner with the noisy target was switched such that each participant fulfilled both the “more skilled” and “less skilled” roles.

Consistent with the simulation, the participants’ tracking performance improvement (Fig. 3B) was also affected by the stiffness scenario (Friedman test, $\chi^2 = 92, p < 0.001$). The LH scenario was found to result in the most improvement [LH

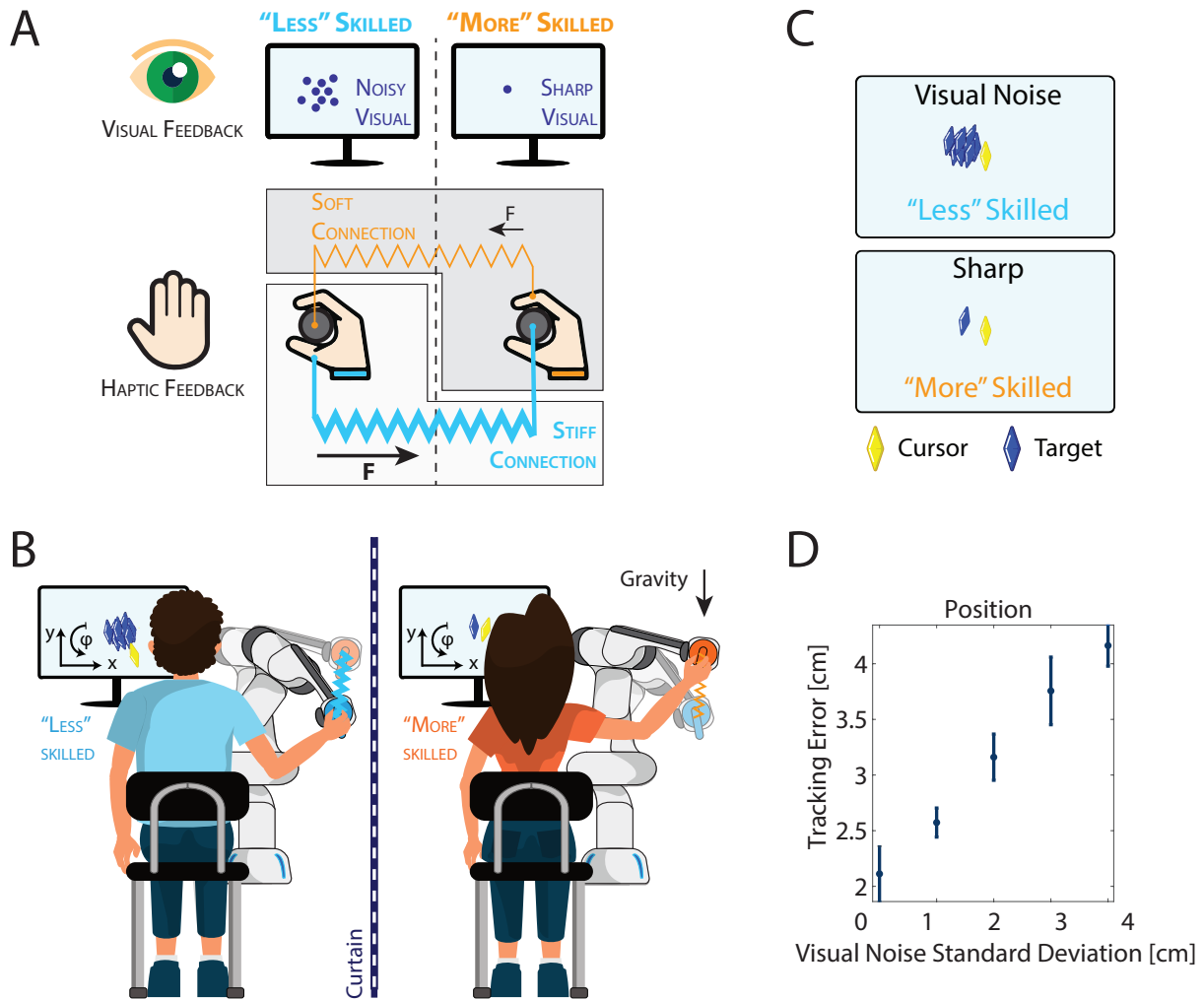


Fig. 1. **Asymmetric connection concept and experiment task.** (A) Concept: The connected partners receive visual and haptic feedback while tracking. The one receiving noisy visual feedback is effectively “less” skilled at the tracking task and receives stronger haptic feedback due to a stiff connection; the one receiving sharp visual feedback is effectively “more” skilled and receives weaker haptic feedback due to a soft connection. (B) Paired participants, separated by a curtain, tracked the same moving target. Each of them was seated in front of a monitor on which the target and their own cursor were displayed. The cursor was controlled by guiding a robot end-effector in the vertical plane. The two robots connected the participants through a virtual elastic band with potentially different stiffness levels for each robot. (C) The target display for the two partners of a dyad, with a single target for the sharp condition and a cloud of ten Gaussian distributed target replicas for the noisy condition. (D) The tracking error increases with the noise magnitude, thus enabling us to degrade the “skill” of one partner. In the experiment we used a standard deviation equal to 0 cm (and 0°) and 2 cm (and 8°), respectively for the “more” and “less” skilled partner.

$> \text{HH} (p < 0.001) > \text{LL} (p = 0.041) > \text{HL} (p < 0.001)$]. The experiment effort A, with α computed as the average muscle activity recorded with EMG sensors on six arm muscles (see Methods), was also impacted by the stiffness scenario (Durbin test, $\chi^2 = 36, p < 0.001$; Fig. 3B). However, while a similar trend to the simulation was observed, the experimental results now found no difference between the LH and LL conditions with $\text{HL} > \text{HH} (p = 0.028) > \text{LH} (p = 0.004) = \text{LL} (p = 1)$.

Finally, the stiffness conditions affected the trade-off values (Friedman test, $\chi^2 = 107, p < 0.001$) both across all participants and when they were separated between more and less skilled participants. For both groups, the asymmetric LH and HL resulted in the highest and lowest value, respectively. However, the symmetric conditions showed opposite results

for different relative participant performance. Here for the less skilled participants the HH scenario allowed better performance than the LL [$\text{LH} > \text{HH} (p = 0.041) > \text{LL} (p < 0.001) > \text{HL} (p < 0.001)$]; the opposite occurred in the more skilled group [$\text{LH} > \text{LL} (p = 0.044) > \text{HH} (p < 0.001) > \text{HL} (p < 0.001)$].

As in the simulated data, we exploited linear-mixed effect models to fit data obtaining R^2 equal to 0.77 (HH), 0.58 (LL), 0.69 (HL), 0.61 (LH) for the improvement and R^2 equal to 0.037 (HH), 0.009 (LL), 0.18 (HL), 0.0012 (LH) for the effort (see *Supplementary Materials* for more details on the parameter fitting).

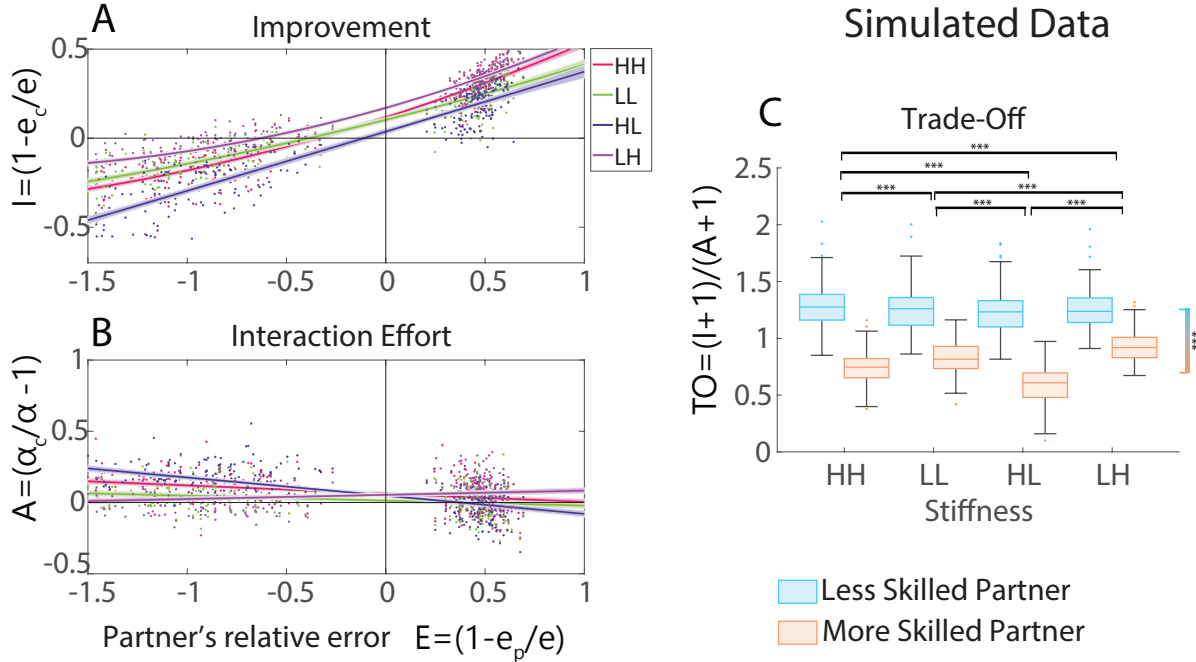


Fig. 2. **Simulated human-human experiment.** Improvement (A) and interaction effort (B) in the three DoFs tracking task (average value among x, y, φ) as a function of the partner's relative error. Each dot corresponds to the data of one trial for one subject, where different colours are used to highlight the four stiffness conditions. The fits obtained from linear mixed-effect models (see Methods) for each condition are depicted with solid lines, where shadows represent confidence intervals. Note that in the LH condition, little increase of effort is required from the more skilled partner, without there being performance degradation. Panel (C) shows the trade-off between improvement and effort for the four stiffness conditions $\{HH, LL, HL, LH\}$. The first stiffness index always refers to the more skilled partner. *** $p < 0.001$

III. DISCUSSION

We studied the mechanisms of haptic communication within a tracking task requiring gravity compensation to evaluate more complex and realistic scenarios than the previously investigated simple one or two DoFs tasks. Our results in a three DoFs task using commercially available Panda robots confirm the benefits of haptic communication on more complex tasks and using different robotic and visual interfaces as in [16], [10], [14], [13], [11]. Critically, the experimental results demonstrate that combining a rigid connection for less skilled partners with a soft one for more skilled partners allows for better tracking with less effort, as was predicted by the computational model.

The model of haptic communication based on the exchange of the motion plan between connected individuals introduced in [14], [13] was extended to predict how individuals would respond to asymmetric stiffness. As hypothesised, providing a more rigid guidance to the worse partner and a soft connection to the better one (the LH case), led to an optimal trade-off between improvement and effort. The dependence on stiffness observed in our experiment corroborates and extends the findings of [13], [17]. Our results showed that tuning differently the interaction in the two directions allows the skilled partner to provide more information and guidance to the less skilled one without increasing the effort to overcome their potential perturbations.

While the improvement results matched previous findings

and simulations, we note that there was a difference between simulated and experimental effort results. In the simulation, a soft symmetric connection (LL case) led to a lower effort than the asymmetric LH case, while no difference was found in the experiment. This difference might be caused by our model not considering co-contraction nor gravity compensation which both likely affected the muscle activity measured by EMG sensors. Indeed, co-contraction has been shown to be used by the more skilled participant to counteract disturbances resulting from the worse partner [17].

In conclusion, by physically connecting individuals via two robotic interfaces that can modulate their interaction, it becomes possible to improve their performance with minimal effort. In particular, using connecting robots or “conbots” to create an asymmetric connection strengthening the influence of the more accurate partner opens opportunities to optimally modulate the physical interaction between partners, maximizing tracking performance without requiring additional effort from the partners relative to solo performance. This can be used in physical training and learning scenarios (see e.g. [18]), where the teacher-student dyads will typically have highly different skills, and in general to practice between partners of different skill, such as two patients or a patient training with e.g. a family member.

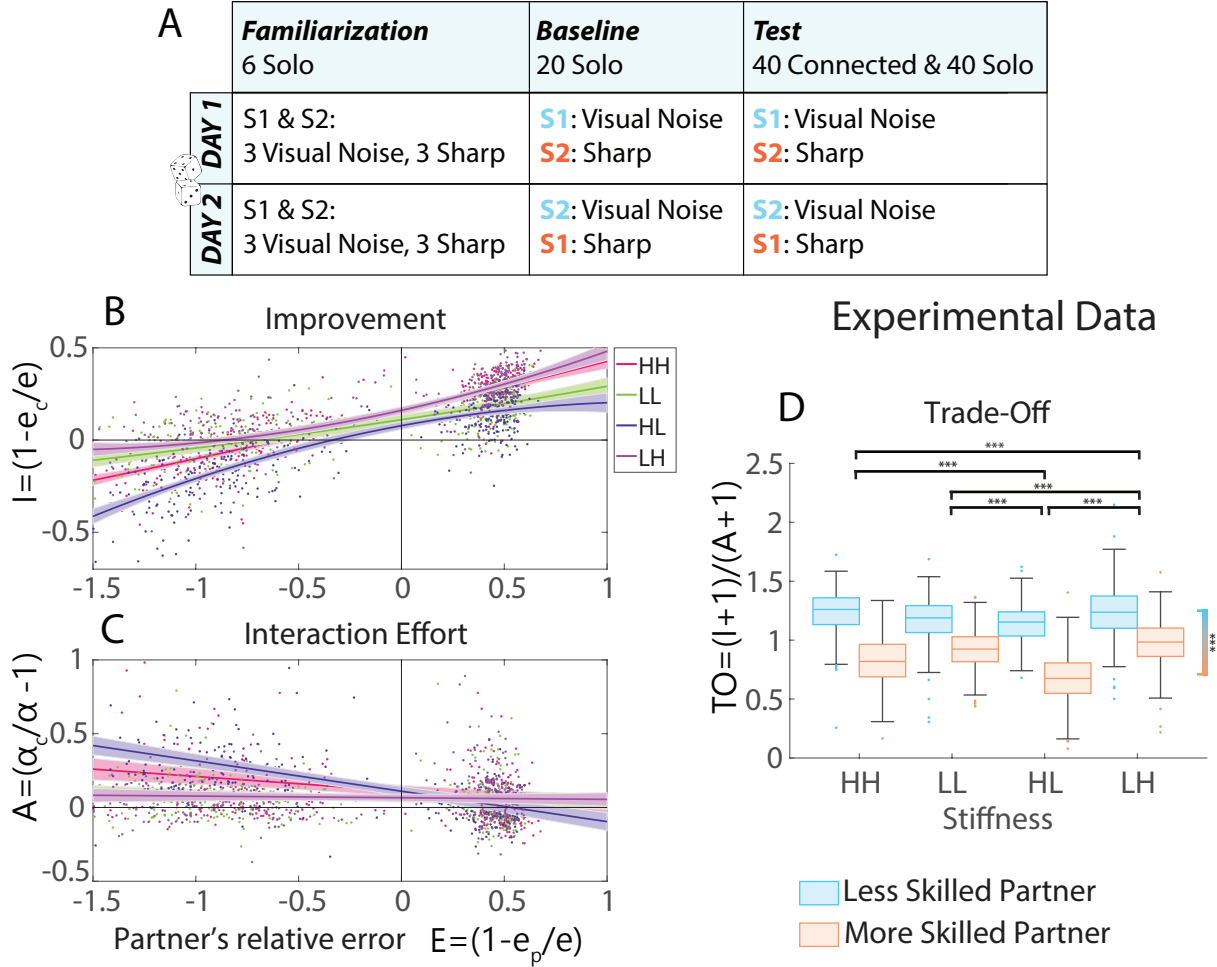


Fig. 3. **Human-human experiment carried out with the same conditions as the simulation.** (A) Experimental Protocol: dyads underwent 2 sessions on two different days (in a random order), each with familiarization, baseline and test phases. Connected trials were with viscoelastic connection, solo trials without. The resulting performance improvement (B), interaction effort (C) and trade-off (D).

IV. MATERIALS AND METHODS

A. Simulation model and protocol

The behaviour of a connected dyad (Fig. 1A) was simulated modelling each individual's actions through the combination of a *motor controller* and an *observer*. The observer consisted of a Kalman filter considering the linear system dynamics

$$\begin{cases} \mathbf{z}(t+1) = \mathbf{A}\mathbf{z}(t) + \mathbf{B}[\mathbf{u}(t) + \mathbf{F}(t)] \\ \mathbf{w}(t+1) = \mathbf{H}\mathbf{z}(t+1), \end{cases} \quad (1)$$

$$\mathbf{A} = \begin{bmatrix} \mathbf{1} & dt\mathbf{1} \\ \mathbf{0} & \mathbf{1} \end{bmatrix}, \quad \mathbf{B} = \begin{bmatrix} \mathbf{0} \\ dt\mathbf{I}^{-1} \end{bmatrix}, \quad \mathbf{H} = \begin{bmatrix} \mathbf{1} & \mathbf{0} \\ \mathbf{1} & \mathbf{0} \end{bmatrix},$$

where $\mathbf{z} = [\mathbf{q}', \dot{\mathbf{q}}']'$ represents the state of each partner's hand, with $\mathbf{q} \equiv [x, y, \varphi]'$ the coordinates of the three DoFs, dt the time step, \mathbf{w} the measurement, \mathbf{F} the interaction force, \mathbf{u} the motor command, \mathbf{I} the inertia, $\mathbf{1}$ the 3×3 identity matrix and $\mathbf{0}$ the 3×3 null matrix. Here, the interaction force \mathbf{F} was given by

$$\mathbf{F} = \mathbf{K}(\mathbf{q}_p - \mathbf{q}) + \mathbf{D}(\dot{\mathbf{q}}_p - \dot{\mathbf{q}}), \quad (2)$$

where p refers to the partner's variables, considered the viscoelastic force/torque resulting from the connection between participants with stiffness \mathbf{K} and damping \mathbf{D} .

The Kalman filter considered the measurement $\mathbf{w} = [\hat{\mathbf{q}}'_v, \hat{\mathbf{q}}'_h]'$ obtained from the participant's visual (v) and haptic (h) feedback, both affected by noise (VN and HN respectively). Here the noise associated with the haptic information is composed of the coupled effect of their partner's visual noise and the stiffness-dependent impact of communication over a haptic channel (i.e., the higher the stiffness connection, the lower the noise). These noise components are expressed, for the subject $i \in \{1, 2\}$, through the covariance matrix

$$\mathbf{R}_i = \begin{bmatrix} VN_i & 0 \\ 0 & VN_j + HN_i \end{bmatrix}, \quad (3)$$

where $j \in \{1, 2\}$ and $j \neq i$ indicates the other partner. VN_i is the standard deviation of the visual noise affecting the target for subject i , VN_j the standard deviation of the visual noise affecting the target for subject j , and HN_i defines the noise over the haptic information of the subject i , which is related to the connection stiffness.

The motor controller for each participant determined the motor command \mathbf{u} through the linear control law

$$\mathbf{u} = \mathbf{L}'(\hat{\mathbf{z}}^* - \mathbf{z}), \quad (4)$$

where \mathbf{L} denotes the control gain and $\hat{\mathbf{z}}^*$ their estimate of the target state obtained through a Kalman filter. In the present work we provided the Kalman filters of the two subjects with the same information about the target, i.e., we did not considered a second Kalman filter for the estimate of the target's partner as in [13]. \mathbf{L} was obtained by minimising the quadratic cost composed of the participants' error and effort such that

$$J = \int_{t=0}^{\infty} e' Q e + u' R u dt, \quad (5)$$

where the error cost matrix and effort cost matrix were set as $Q = \text{diag}(25, 200)$ and $R = 0.01$ when considering the translational DoFs and $Q = \text{diag}(10^4, 8 \cdot 10^3)$ and $R = 10^{-8}$ when considering the orientation DoF.

The inertia, stiffness and damping parameters were estimated from the real experiment system (Panda robot + human arm) and accordingly set as

$$\mathbf{I} = \begin{bmatrix} 2.917 & 0 & 0 \\ 0 & 6.257 & 0 \\ 0 & 0 & 0.0026 \end{bmatrix} \text{ kg m}^2,$$

$$\mathbf{K} = \begin{bmatrix} K_x & 0 & 0 \\ 0 & K_y & 0 \\ 0 & 0 & K_\varphi \end{bmatrix},$$

$$\mathbf{D} = 0.005 \begin{bmatrix} \sqrt{K_x} & 0 & 0 \\ 0 & \sqrt{K_y} & 0 \\ 0 & 0 & \sqrt{K_\varphi} \end{bmatrix}.$$

Depending on the stiffness scenario, the stiffness matrix \mathbf{K} was set high (H: $\{K_x = K_y = 180 \text{ N/m}, K_\varphi = 9 \text{ Nm/rad}\}$), low (L: $\{K_x = K_y = 60 \text{ N/m}, K_\varphi = 3 \text{ Nm/rad}\}$) or null for solo trials.

Two preliminary experiments were conducted to estimate the mapping from participant i -th tracking errors to the amount of visual noise (VN_i) and connection stiffness (HN_i). In both experiments we evaluated the performance of individuals executing three DoFs tracking tasks while receiving different noise. This considered different amounts of visual feedback noise -four noise levels plus a no-noise condition- or haptic feedback {low or high} stiffness connection with the target. During the task, participants could only use the provided visual or haptic feedback (details on these experiments can be found in *Supplementary Materials*).

A total of 160 trials were simulated, where the 30 s target trajectory was set to a multi-sine for all the DoFs such that

$$\begin{cases} x(t) = 6.4 \sin(1.8t) + 2.5 \sin(1.82t) + 4.3 \sin(2.34t) \\ y(t) = 3 \sin(1.1t) + 3.2 \sin(3.6t) + 3.8 \sin(2.5t) \\ \quad + 4.8 \sin(1.48t) \\ \phi(t) = 20 \sin(1.4t) + 12 \sin(2.5t) + 17.5 \sin(1.8t) \\ \quad + 8.1 \sin(2t). \end{cases} \quad (6)$$

Symmetric and asymmetric conditions were tested for the haptic connection, through the four conditions {HH, LL, HL, LH}. Individual skill levels were simulated as in [13] by varying the amount of visual noise, within two ranges leading to lower/higher errors (2–3.7 cm and 3.8–7 cm in terms of position and 6° – 8° and 9° – 13° in terms of orientation) as described in the results of the preliminary Visual Noise experiment (see Fig. 1D and *Supplementary Materials*)

Human-human experiment

The study was approved by the Ethics Committee of Università Campus Bio-Medico di Roma (HUROB protocol) and carried out in accordance with the Declaration of Helsinki. 20 healthy volunteers (aged 22.5 ± 2.6 years old, 9 female, 18 right-handed) participated in the experiment after providing written informed consent. Participants were randomly organized in ten dyads, where members of each dyad had the same handedness (assessed through the Oldfield test [15]).

Each dyad's partner sat in front of a monitor displaying a randomly moving target and a cursor corresponding to their hand movement while being connected to a robotic interface (see Fig. 1B). A common reference system, centred in the monitor centre, was used where cursor translations corresponded to twice the physical translations, to let participants reach the entire virtual workspace with feasible arm movements. Partners were haptically connected through a visco-elastic force/torque \mathbf{F} that was the same as that employed in simulation eq. (2). A curtain separated the paired individuals hiding their partner and setup. Participants were informed that they may encounter some force on the handle but were not advised of the task performed by the partner nor of a possible physical connection with them.

Each participant was required to track a target constrained to the three DoFs $\{x, y, \varphi\}$ in the vertical plane in front of them with a diamond-like cursor by moving an ergonomic handle fixed to the robot end-effector (Fig. 1B). The target moved with the multi-sine trajectory eq. (6), where an offset (x_0, y_0, φ_0) was added so that for each trial, t started from a randomly selected zero $\{t_0 \in [0, 30]s, x(t_0) \equiv y(t_0) \equiv \phi(t_0) \equiv 0\}$ of the multi-sine trajectory, to minimize memorization. Overall, the target was within a $26 \times 26 \text{ cm}^2$ square workspace in the virtual reference system, with a maximum rotation of $\pm 55^\circ$ with respect to the vertical axis.

The robotic interface (Panda by Franka Emika) constrained the motion to the translation and rotation in the vertical plane. To this aim, the robot was impedance controlled with low impedance (i.e., "transparent" behaviour) along the task directions and high impedance along the constrained directions. The robot torque vector was computed as $\boldsymbol{\tau} = \mathbf{J}'[\mathbf{K}_c \mathbf{e} - \mathbf{D}_c(\mathbf{J}\dot{\mathbf{q}})] + \nu \mathbf{B}\dot{\mathbf{q}} + \mathbf{C} + \mathbf{g}$, where \mathbf{K}_c and \mathbf{D}_c are diagonal 6×6 matrices representing the stiffness and damping elements, $\dot{\mathbf{q}}$ is the joint velocity vector and \mathbf{J} is the 6×7 Jacobian matrix. \mathbf{B} is the residual damping matrix in the joint space, previously estimated to compensate the damping of each robot joint (see *Supplementary Materials*), $\nu = 0.8$, \mathbf{C} and \mathbf{g} represent the Coriolis and gravity contributions. $\mathbf{e} = \mathbf{p}_d - \mathbf{p}_a$ is the pose error between the 6×1 desired (\mathbf{p}_d) and the 6×1 actual (\mathbf{p}_a)

end-effector pose vectors. The diagonal components of \mathbf{K}_c along the constrained directions were set to 150 N/m and 20 Nm/rad for translational and rotational terms, respectively. Along those directions, the desired pose \mathbf{p}_d was set equal to the initial one, i.e., the centre of the task workspace. Whereas, along the task directions ($\{y, z, \varphi\}$ in robot base frame), the stiffness components were set null in the solo trials, that is the subject does not feel any interaction force. Along the same directions, in the coupled trials, the stiffness was set accordingly to the protocol and \mathbf{p}_d is the actual pose of the partner, so that $\mathbf{p}_d^1 = \mathbf{p}_a^2$ and $\mathbf{p}_d^2 = \mathbf{p}_a^1$, with the superscript 1 and 2 referring to the two partners.

The handle pose and velocity were estimated and recorded by means of robot encoders and kinematic computation. Surface electromyography (EMG) sensors (TrignoTM Wireless System, Delsys) were employed to measure the muscle activity of three arm flexors and three extensors involved in the task: Pectoralis major, Posterior deltoid, Biceps brachii, Lateral head of triceps brachii, Flexor carpi radialis, Extensor carpi radialis longus.

To test partners with a range of different relative skill levels, the individuals' skill to carry out the task was modulated through the addition of Gaussian visual noise on the target (see Fig. 1C) of one partner per dyad [13]. In particular, in the noisy condition the single target was replaced by a cloud of ten replicas normally distributed around the target pose $-x, y$ and φ with a standard deviation equal to 2 cm for the position (x and y) and 8° for orientation (φ). These values were chosen considering the error for different levels of noise measured in a preliminary *visual noise experiment* (see Fig. 1D and *Supplementary Materials*). To balance the experimental condition, the same 20 participants underwent a second experimental session with the other partner having visual noise. Thus, the overall pool considered in the data analysis was composed of 20 different dyads.

As in simulations, two sessions and four stiffness scenarios were considered ($\{\text{HH, LL, HL, LH}\}$). During each experimental session, dyads underwent 30 s trials (followed by 10 s break to prevent fatigue) in the following three phases:

- 1) *Familiarization*: six *solo* trials (with no physical connection between partners) of which three were with the visual noise and three were with the sharp target, in the same random order for both partners.
- 2) *Baseline*: 20 *solo* trials, with visual noise for one partner only.
- 3) *Test*: 80 alternating *solo* and *connected* trials, all with visual noise for one partner only (the same as the baseline). The four stiffness conditions were randomized among the 40 connected trials, resulting in ten repetitions per condition.

In the second session with the same dyad, the visual noise in the *baseline* and *test* conditions was assigned to the other partner.

Data analysis

Raw EMG signals were filtered using a second-order Butterworth band-pass filter in the 20-450 Hz range and a notch

filter at 50 Hz, then rectified and finally low-pass filtered using a second-order Butterworth filter with a cut-off frequency of 5 Hz.

The filtered EMG data of each sensor was averaged over time for each trial. Then, *connected* trial data was normalized with respect to the value obtained from the previous *solo* trial. The root mean square among normalized data of all the sensors was used as an estimation of the effort. Since the first trial of the *task* block was *connected*, the EMG value of such block was normalized with the last trial of the *baseline*.

The tracking error was computed as the difference between the target and the cursor separately along x , y and ϕ . The root mean square of each error metric was computed along each trial and then used to calculate the performance metrics, i.e., the *performance improvement* (I), the *interaction effort* (A) and the *partner's relative error* (E), as described in the Results section. All the metrics were computed separately for each DoF and then averaged.

Linear mixed-effect models were used to fit with a first/second-order polynomial respectively the effort and the improvement with respect to the partner's relative error, for each stiffness condition from $\{\text{HH, LL, HL, LH}\}$. In particular, the relationship between *improvement* I and *partner's relative error* E was investigated employing a linear mixed-effect model with I as the dependent variable, E and E^2 as predictors, and dyads as random effect, considering both E and I the averaged value among the three DoFs, as follows:

$$I = \beta_0 + \beta_1 E + \beta_2 E^2 + \varepsilon_I, \quad (7)$$

where ε_I is the unexplained variance term associated with each analysed dyad, considering the same 'physical couple' with inverted noise conditions as two different dyads. A similar analysis was carried out to fit the *Effort* A with respect to the *partner's relative error* E , considering this metric as a predictor:

$$A = \delta_0 + \delta_1 E + \varepsilon_A. \quad (8)$$

Model simulation and data analysis were conducted on Matlab 2020. The goodness of fitting was evaluated through R^2 and p values for the intercept and coefficients estimates. Statistical analysis was performed using Jasp 0.16 [19]. After having assessed the non-normality of the data through the Shapiro-Wilks test, the Friedman test was employed to compare the above-mentioned metrics, with the individual skill (i.e., less or more skilled) and the stiffness condition (i.e., $\{\text{HH, LL, HL, LH}\}$) as main factors. Post-hoc analysis was conducted using paired Wilcoxon test with the Bonferroni correction.

SUPPLEMENTARY MATERIALS

Details on the model parameter identification, preliminary experiments and additional analysis and results can be found in *Supplementary Materials*.

ACKNOWLEDGMENT

This work was supported by the European Commission under H2020 grant CONBOTS (ICT 871803).

Competing Interests: The authors declare that they have no competing interests.

Ethics Approval: The study was approved by the Ethics Committee of Università Campus Bio-Medico di Roma (HUROB protocol) and carried out in accordance with the Declaration of Helsinki.

Consent to participate: Informed consent was obtained from participants after the nature and possible consequences of the studies were explained.

Data availability: All data needed to evaluate conclusions in the paper are available at the Data Repository (10.5281/zenodo.10391532).

Author contributions: A.N., S.B., G.D.P., E.B., N.D.S. and D.F. contributed to the conception of the work; A.N., S.B. and D.F. designed the study; A.N, S.B., J.E and X.C. implemented the model; A.N. and S.B. developed the experimental setup, collected and analyzed data. All authors contributed to the interpretation of the results and to the paper drafting.

REFERENCES

- [1] N. Sebanz, H. Bekkering, and G. Knoblich, "Joint action: bodies and minds moving together," *Trends In Cognitive Sciences*, vol. 10, no. 2, pp. 70–76, 2006.
- [2] A. Sawers and L. H. Ting, "Perspectives on human-human sensorimotor interactions for the design of rehabilitation robots," *Journal of Neuro-engineering and Rehabilitation*, vol. 11, pp. 1–13, 2014.
- [3] S. Gentry, E. Feron, and R. Murray-Smith, "Human-human haptic collaboration in cyclical fitts' tasks," *IEEE/RSJ International Conference on Intelligent Robots and Systems*, pp. 3402–3407, 2005.
- [4] K. B. Reed and M. A. Peshkin, "Physical collaboration of human-human and human-robot teams," *IEEE Transactions on Haptics*, vol. 1, no. 2, pp. 108–120, 2008.
- [5] N. Stefanov, A. Peer, and M. Buss, "Role determination in human-human interaction," *World Haptics, Joint EuroHaptics conference and Symposium on Haptic Interfaces for Virtual Environment and Teleoperator Systems*, pp. 51–56, 2009.
- [6] D. Feth, R. Groten, A. Peer, S. Hirche, and M. Buss, "Performance related energy exchange in haptic human-human interaction in a shared virtual object manipulation task," *World Haptics, Joint EuroHaptics conference and Symposium on Haptic Interfaces for Virtual Environment and Teleoperator Systems*, pp. 338–343, 2009.
- [7] R. Groten, D. Feth, H. Goshy, A. Peer, D. A. Kenny, and M. Buss, "Experimental analysis of dominance in haptic collaboration," *RO-MAN, The IEEE International Symposium on Robot and Human Interactive Communication*, pp. 723–729, 2009.
- [8] R. P. Van der Wel, G. Knoblich, and N. Sebanz, "Let the force be with us: dyads exploit haptic coupling for coordination," *Journal of Experimental Psychology: Human Perception and Performance*, vol. 37, no. 5, p. 1420, 2011.
- [9] C. Basdogan, C.-H. Ho, M. A. Srinivasan, and M. Slater, "An experimental study on the role of touch in shared virtual environments," *ACM Transactions on Computer-Human Interaction (TOCHI)*, vol. 7, no. 4, pp. 443–460, 2000.
- [10] G. Ganesh, A. Takagi, R. Osu, T. Yoshioka, M. Kawato, and E. Burdet, "Two is better than one: Physical interactions improve motor performance in humans," *Scientific Reports*, vol. 4, no. 1, pp. 1–7, 2014.
- [11] N. Beckers, E. H. van Asseldonk, and H. van der Kooij, "Haptic human-human interaction does not improve individual visuomotor adaptation," *Scientific Reports*, vol. 10, no. 1, pp. 1–11, 2020.
- [12] E. Ivanova, J. Eden, G. Carboni, J. Krüger, and E. Burdet, "Interaction with a reactive partner improves learning in contrast to passive guidance," *Scientific Reports*, vol. 12, no. 1, p. 15821, 2022.
- [13] A. Takagi, F. Usai, G. Ganesh, V. Sanguineti, and E. Burdet, "Haptic communication between humans is tuned by the hard or soft mechanics of interaction," *PLoS Computational Biology*, vol. 14, no. 3, p. e1005971, 2018.
- [14] A. Takagi, G. Ganesh, T. Yoshioka, M. Kawato, and E. Burdet, "Physically interacting individuals estimate the partner's goal to enhance their movements," *Nature Human Behaviour*, vol. 1, no. 3, 2017.
- [15] R. C. Oldfield, "The assessment and analysis of handedness: The edinburgh inventory," *Neuropsychologia*, vol. 9, no. 1, pp. 97–113, 1971.
- [16] K. Reed, M. Peshkin, M. J. Hartmann, M. Grabowecky, J. Patton, and P. M. Vishton, "Haptically linked dyads: are two motor-control systems better than one?" *Psychological Science*, vol. 17, no. 5, pp. 365–366, 2006.
- [17] H. Börner, G. Carboni, X. Cheng, A. Takagi, S. Hirche, S. Endo, and E. Burdet, "Physically interacting humans regulate muscle coactivation to improve visuo-haptic perception," *Journal of Neurophysiology*, vol. 129, no. 2, pp. 494–499, 2023.
- [18] "Conbots: connected through robots," 2020, <https://www.conbots.eu/> [Accessed: 28-June-2023].
- [19] JASP Team, "JASP (Version 0.16.4)[Computer software]," 2022. [Online]. Available: <https://jasp-stats.org/>

Supplementary Materials

Robot-mediated asymmetric connection between humans can improve performance without increasing effort

Alessia Noccaro^{1,2†*}, Silvia Buscaglione^{2†}, Jonathan Eden^{3,4}, Cheng Xiaoxiao³, Nicola Di Stefano⁵, Giovanni Di Pino², Etienne Burdet³, and Domenico Formica^{1,2*}

¹Neurorobotics Lab, School of Engineering, Newcastle University, UK

²NEXT: Neurophysiology and Neuroengineering of Human-Technology Interaction Research Unit, Università Campus Bio-Medico di Roma, Italy.

³ Department of Bioengineering, Imperial College of Science Technology and Medicine, London, UK.

⁴ Mechanical Engineering Department, University of Melbourne, Victoria, Australia,

⁵ Institute of Cognitive Sciences and Technologies (ISTC), National Research Council (CNR), Rome, Italy

† Equal contribution

* E-mail: {alessia.noccaro, domenico.formica}@newcastle.ac.uk

MODEL PARAMETER IDENTIFICATION

Human motor performance with/without a physical connection was simulated by extending the haptic communication model of [1] as described in the Methods section and depicted in Fig. S1.

We conducted two preliminary experiments to estimate the model parameters that relate the tracking error to the amount of visual noise (*Visual Noise Experiment*) and connection stiffness (*Haptic Control Experiment*), respectively. In both experiments participants performed a tracking task in the same configuration used for the main experiment.

The protocols were approved by the Ethic Committee of Università Campus Bio-Medico di Roma and carried out according to Helsinki Declaration. The participant groups of the two experiments were different among them. All participants performed one of these experiments after providing written informed consent. The average tracking error, in terms of position and orientation, resulting from the variation of the visual noise standard deviation and the connection stiffness, is shown in Fig. S2.

Visual noise experiment

Six healthy volunteers (all right-handed, aged 30.7 ± 6.9 , 3 female), were asked to execute 50 trials of a three DoFs tracking task in the solo condition. Five different levels of Gaussian noise (including no noise) were added to the target and randomly presented to the participants. The values of standard deviation (SD) associated to i^{th} noise level for position p and orientation ϕ were computed as: $SD|_{p,i} = i$ cm and $SD|_{\phi,i} = i 4^\circ$, where $i \in \{0, 1, 2, 3, 4\}$.

Using the results observed in the experiment of [2] (see Fig. S2A and Fig. S2B), we chose to use the second noise

level ($i = 2$) as the noisy target condition in our main experiment. This noise level was chosen as it produced an average error of about 10% of the target range of motion for both position and orientation.

Haptic control experiment

As in the study [1], we conducted a *haptic control experiment* to model the effect that the connection stiffness had on the received haptic information. Eight healthy volunteers (all right-handed, 31.2 ± 2.6 years old, 3 females) participated in this experiment and were required to execute the same three DoFs tracking task as used in the main experiment. Different to the main experiment, only their cursor (and not the target) was displayed on the monitor, where the target information could only be understood through their connection to a virtual spring along the 3 DoFs involved in the task. The stiffness value of the rotational and linear springs was set high (H) for the first ten trials and low (L) for the last ten trials, considering the stiffness values used in the model and main experiment.

The results of this experiment, shown in Fig. S2C and S2D, provide the relationship between the connection stiffness and the conveyed haptic information, measured through tracking performance. The obtained equations were used for the computation of HN used in eq. (3) in the manuscript.

ADDITIONAL ANALYSIS ON PERFORMANCE DATA

To understand the effect of the participant's relative ability on their performance, we separated the data according to the participants' skill i.e., their visual noise condition (noisy vs sharp target). From Fig. S3B it can be seen that the less skilled partner (with the noisy target) improves in the HH

and LH more than in the other conditions ($p < 0.001$), and the converse holds for the more skilled partner (sharp target) whose improvement is lower ($p < 0.001$) in the HH and HL than in the LL or LH conditions. Additionally, LH is the only condition with no observed performance deterioration ($I < 0$; $p = 0.825$) for the more skilled individual (HH,HL: $p < 0.001$; LL: $p = 0.007$).

The more skilled partners were also found to require more interaction effort in the HH and HL conditions (Fig. S3B). Moreover, their effort was significantly higher ($p < 0.001$) than the less skilled partners' effort in all cases except for the LH condition where they are balanced ($p = 0.89$).

The average joint behaviour considering both members of a dyad was also evaluated. Here, the average improvement within dyads (Fig. S3C) was observed to be larger ($p < 0.001$) in the LH condition than in all other conditions, with no clear difference between the HH and LL conditions. Moreover, the average dyad effort (Fig. S3D) was lower in the LH condition ($p < 0.001$) than in the other conditions, except for LL. These results further demonstrate the LH condition allows for the highest participant improvement with the smallest amount of effort across the dyad.

MIXED-EFFECT MODEL DATA FITTING

As in [1], a second-order linear mixed-effect model was employed to describe the relation between *improvement* I and *partner's relative error* E (see equation 7), where I was set as the dependent variable, E and E^2 as the predictors. Both E and I were considered as the averaged values among all three DoFs.

A similar first-order linear mixed model has been exploited to investigate the relation between *Partner's Relative Error* E and *Effort* A (see eq. 8 in the main text), with A as the dependent variable and E as the predictor. In both models the dyads were considered as a random effect. The obtained fitting results are reported in Table S1 and S2.

REFERENCES

- [1] A. Takagi, F. Usai, G. Ganesh, V. Sanguineti, and E. Burdet, "Haptic communication between humans is tuned by the hard or soft mechanics of interaction," *PLoS Computational Biology*, vol. 14, no. 3, p. e1005971, 2018.
- [2] A. Nocco, S. Buscaglione, G. Di Pino, and D. Formica, "Visual noise linearly influences tracking performance," *Annual International Conference of the IEEE Engineering in Medicine & Biology Society (EMBC)*, pp. 794–797, 2022.

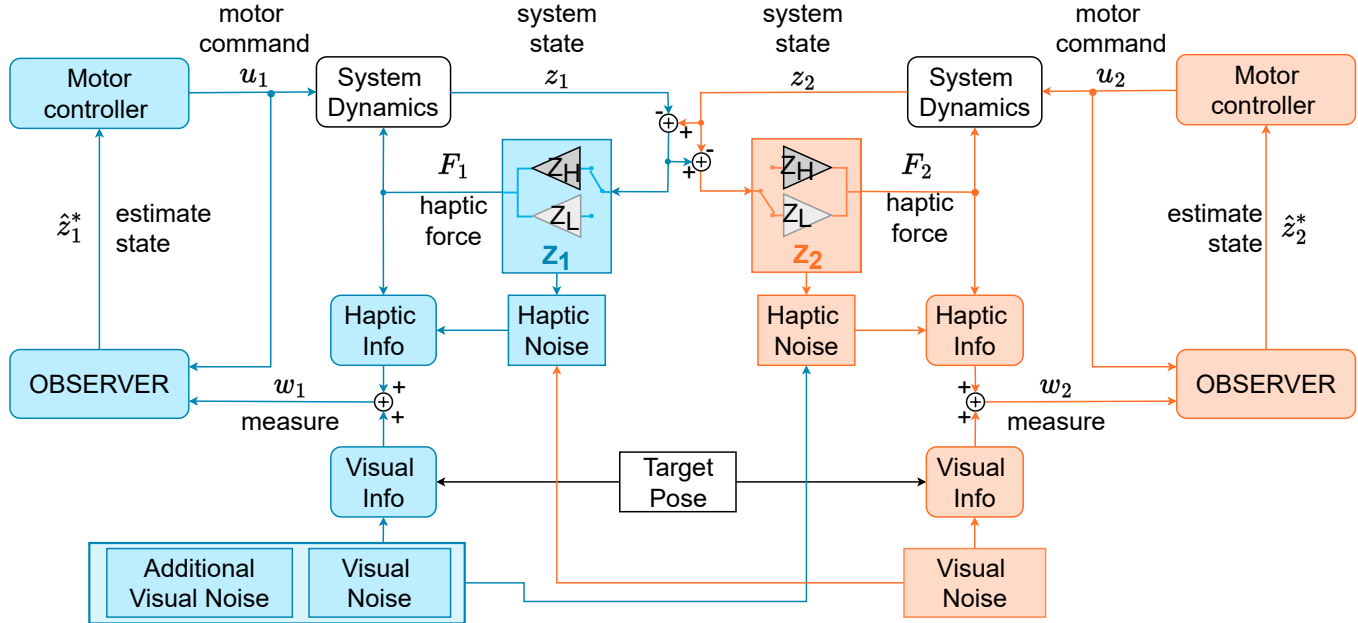


Fig. S1. **Scheme of the haptic communication model between two physically connected individuals in a common tracking task.** Each partner is identified by a colour and schematized as the combination of a *motor controller* and an *observer*. The two partners are connected through a connection stiffness (Z) that can be high or low to model both the symmetric (HH, LL) and asymmetric (HL, LH) conditions. The *motor controller* generates the motor commands $u = Lz^*$ acting on the external system, according to the system state estimate z^* obtained from the *observer*. Here, the estimate derives from an internal model and it is corrected with a Kalman Filter using the motor command and the system measures w obtained from haptic and visual information. The internal model represents the estimation of the environment made by the human brain and corresponds to the dynamic model of the real system (see eq. (1) in the manuscript), assuming that the internal model matrices (\tilde{A}, \tilde{B}) are correct, such that $\tilde{A} = A, \tilde{B} = B$. The visual information of both partners is influenced by a base noise due to the human sensory estimation error. For one subject an additional visual noise is added to increase the performance difference within the dyad. The haptic information is characterized by a haptic noise depending on the rigidity of the connection -indicating how much the received information is clear- and by the visual noise of the partner -indicating the reliability of the received information.

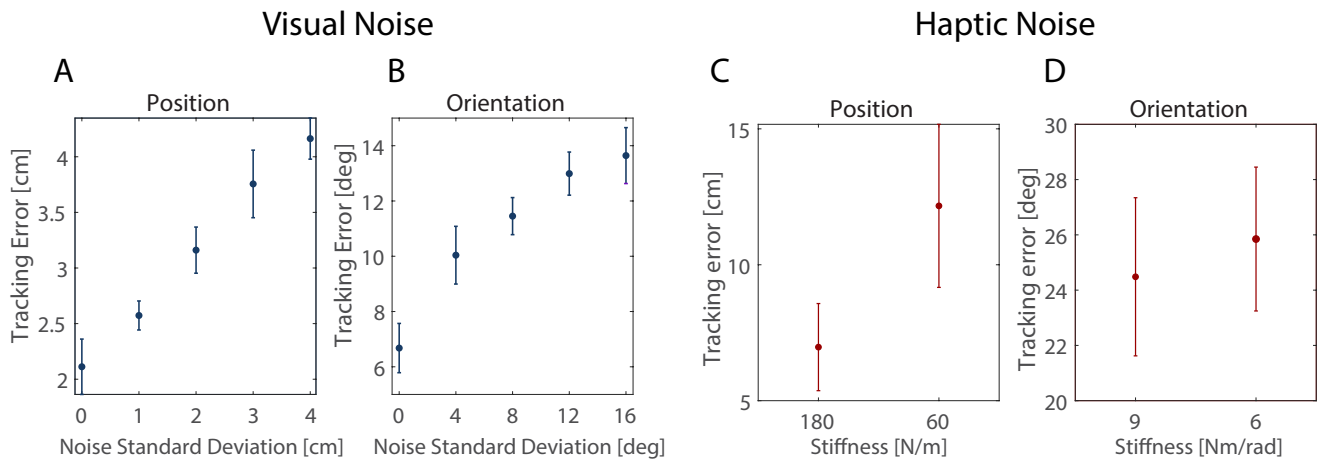


Fig. S2. **Tracking error evaluated for position and orientation for the visual noise and haptic control experiments.** The error in position (A) and orientation (B) are shown for different standard deviations of the target visual noise, where 0 represents the no-noise condition with a single sharp target. Similarly, the position (C) and orientation (D) are shown with respect to the connection stiffness between the cursor and the target when only haptic feedback was provided for the target position.

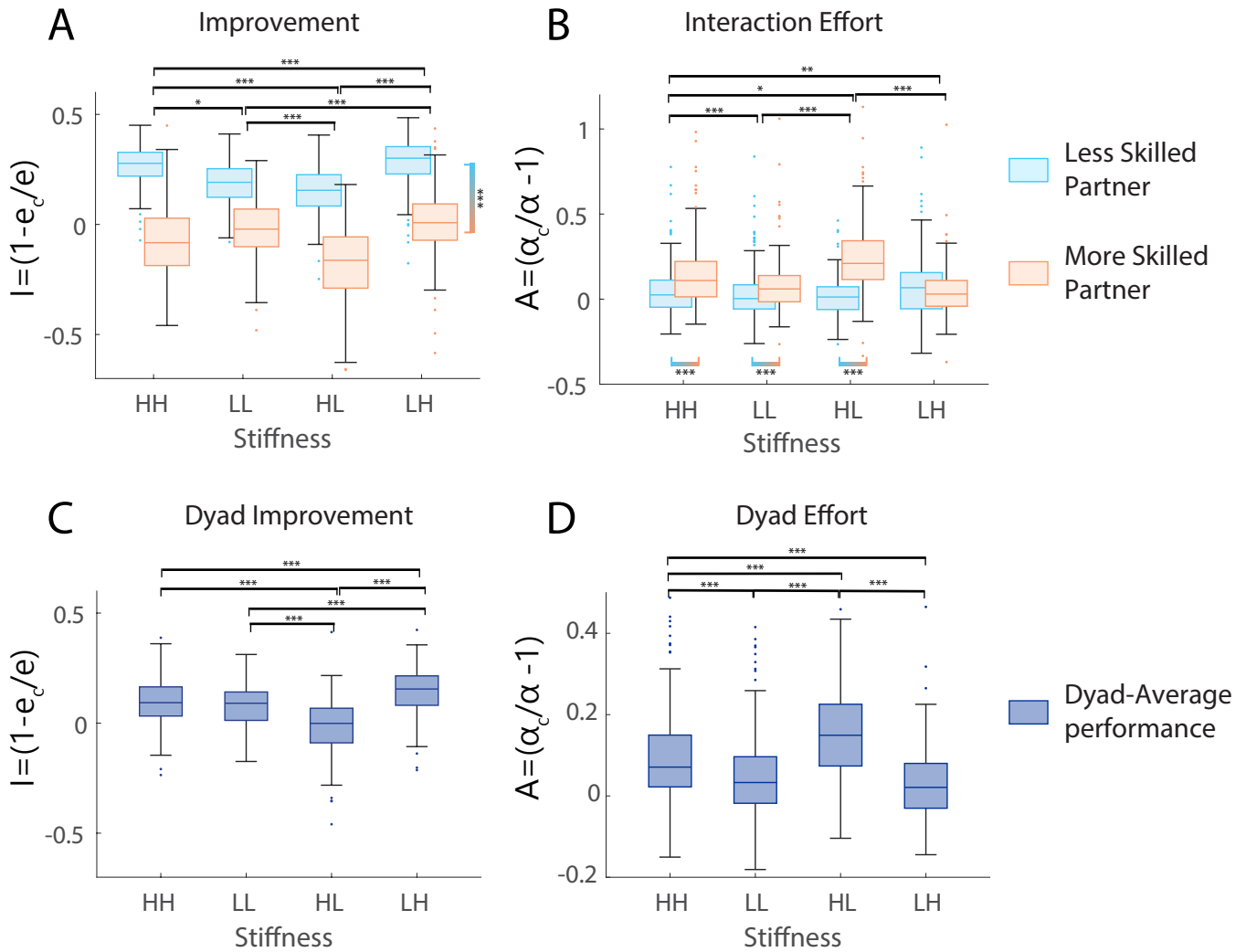


Fig. S3. Improvement (A) and interaction effort (B) in the four stiffness conditions (HH, LL, HL, LH), represented in light blue for people performing with visual noise (less skilled partner) and in orange for their partners with no visual noise (more skilled participants). Average improvement (C) and effort (D) within each dyad for the four stiffness conditions. The first stiffness index always refers to the more skilled partner. * $p < 0.05$, ** $p < 0.01$, *** $p < 0.001$

TABLE S1
IMPROVEMENT DATA FITTING PARAMETERS FOR THE SIMULATED AND EXPERIMENTAL DATA.

Stiffness Condition	Simulated Data				Experimental Data			
	R^2	Parameter	Slope	p -value	R^2	Parameter	Slope	p -value
HH	0.91	Intercept	0.11	< 0.001	0.77	Intercept	0.15	< 0.001
		E	0.36	< 0.001		E	0.26	< 0.001
		E^2	0.060	< 0.001		E^2	0.012	0.38
LL	0.87	Intercept	0.10	< 0.001	0.58	Intercept	0.013	< 0.001
		E	0.28	< 0.001		E	0.17	< 0.001
		E^2	0.031	< 0.001		E^2	0.014	0.36
HL	0.87	Intercept	0.037	< 0.001	0.69	Intercept	0.078	< 0.001
		E	0.33	< 0.001		E	0.21	< 0.001
		E^2	0.85	0.0020		E^2	-0.081	< 0.001
LH	0.93	Intercept	0.17	< 0.001	0.61	Intercept	0.16	< 0.001
		E	0.32	< 0.001		E	0.25	< 0.001
		E^2	0.074	< 0.001		E^2	0.072	< 0.001

TABLE S2
EFFORT DATA FITTING PARAMETERS FOR THE SIMULATED AND EXPERIMENTAL DATA.

Stiffness Condition	Simulated Data				Experimental Data			
	R^2	Parameter	Slope	p -value	R^2	Parameter	Slope	p -value
HH	0.17	Intercept	0.062	< 0.001	0.034	Intercept	0.053	< 0.001
		E	-0.058	< 0.001		E	-0.14	< 0.001
LL	0.076	Intercept	0.013	0.023	0.0070	Intercept	-0.0033	0.46
		E	-0.035	< 0.001		E	-0.079	< 0.001
HL	0.49	Intercept	0.048	< 0.001	0.18	Intercept	0.0079	< 0.001
		E	-0.13	< 0.001		E	-0.24	< 0.001
LH	0.052	Intercept	0.054	< 0.001	-0.0013	Intercept	0.017	0.004
		E	0.030	< 0.001		E	-0.037	< 0.001